

International Journal of Heat and Technology

Vol. 43, No. 5, October, 2025, pp. 1711-1726

Journal homepage: http://iieta.org/journals/ijht

Thermo-Hydraulic Performance Evaluation of Tubular Heat Exchanger Equipped with Variable Diameter Helical Coils



Shodhan Uday Mayekar* Milind Shashikant Yadav

Department of Mechanical Engineering, Hope Foundation's Finolex Academy of Management and Technology, Ratnagiri 415639, India

Corresponding Author Email: shodhanmayekar4@gmail.com

Copyright: ©2025 The authors. This article is published by IIETA and is licensed under the CC BY 4.0 license (http://creativecommons.org/licenses/by/4.0/).

https://doi.org/10.18280/ijht.430510

Received: 19 July 2025 Revised: 15 September 2025 Accepted: 23 September 2025 Available online: 31 October 2025

Keywords:

heat transfer enhancement, variable diameter helical coils, Nusselt number, friction factor, thermal performance factor, response surface methodology

ABSTRACT

This work reports an experimental study on the thermo-hydraulic behavior of a tubular heat exchanger fitted with variable-diameter helical coils. Three coil arrangements, namely convergent, convergent-divergent and divergent, were examined under constant heat flux to determine their influence on heat transfer and flow resistance. The investigation considered the effects of conical length ratio (CLR = 2, 3, 4), diameter ratio (DR = 0.12, 0.16, 0.20), and Reynolds number (Re = 4000 - 10000). Performance was evaluated in terms of the Nusselt number (Nu), friction factor (f), and thermal performance factor (TPF). All coil configurations enhanced heat transfer compared to a plain tube, with average Nu improvements of 37.13%-74.17% for convergent coils, 47.18%-88.18% for convergentdivergent coils, and 58.11%–100.79% for divergent coils. The corresponding increase in f ranged from 1.98-2.97, 2.55-3.80, and 3.22-4.55 times, respectively. Among the three, divergent coils delivered the greatest improvement. A larger DR and smaller CLR promoted Nu enhancement but resulted in greater flow resistance. As TPF values exceeded unity in all cases, variable-diameter coils demonstrated significant potential for heat transfer augmentation. Using Response Surface Methodology (RSM), the optimal parameters were identified as CLR = 2, DR = 0.2, and Re = 10000. The novelty of this work lies in combining variable-diameter coil geometries with RSM-based optimization to generate new insights and practical guidelines for performance improvement of the heat exchanger.

1. INTRODUCTION

In recent years, the rising population, expanding industrial activities, and accelerating urbanization have collectively led to higher energy demand [1]. Clean energy utilization and efficiency improvements are becoming a major focus. At the same time, enhancing the performance of current heat transfer systems remains an active area of research. Heat exchangers are ubiquitous as they find use in chemical and food industries, petrochemical processing, pharmaceutical drug development, refrigeration and waste heat recovery devices [2, 3]. The energy-efficient heat exchangers help to scale down surfacearea requirement, minimize material cost, and reduce weight. Further improving heat exchanger performance also addresses the concern of global energy sustainability.

Making the heat exchanger efficient by increasing the heat transfer coefficient is termed heat transfer augmentation. Different techniques of heat transfer enhancement typically increase the heat duty of a heat exchanger and allow for closer approach temperatures. Various heat augmentation techniques are grouped into two main types-passive and active. Passive techniques do not require any power for their functioning. They depend on modifying the geometry of the tube carrying the fluid or changing the flow physics. These techniques

include the use of inserts [4-9], rough surfaces [10-13], extended surfaces [14-16], etc. Conversely, active methods require external power to operate. The power is imparted to either a heated surface or to fluids. These methods include the use of electric or magnetic fields, fluid or surface vibration, mechanical aids, etc. [17, 18]. By and large, active methods are more intricate and expensive. Hence, they are typically not utilized extensively. However, they come up with an opportunity to regulate the heat transfer enhancement.

Inserts, often called turbulators, offer a cost-effective means of enhancing heat transfer compared to redesigning or replacing the entire heat exchanger. They can be retrofitted into existing systems with minimal modifications. Helical wire coils are recognized as an effective passive method for intensifying the heat transfer and are often applied to improve the thermal performance of heat exchangers [19]. Significant advancements have been made in the past two decades in studying the contribution of wire coil inserts towards heat transfer enhancement of heat exchangers. Garcia et al. [20] experimentally demonstrated the thermo-hydraulic behavior of a round pipe containing helical wire coil inserts in three different regimes of the flow, namely laminar, transition, and turbulent. The effect of pitch and diameter of coil on heat transfer characteristics was described in detail. Effects of coil-

wire inserts with different coil pitches on the heat transfer and pressure drop characteristics in a horizontal double pipe using air as the working fluid were investigated by Naphon [21]. The findings revealed that an increased heat transfer rate was offered by a shorter pitch length. A comparative study of the heat transfer intensification between the tube heat exchanger with wire coil having square and circular shapes in the turbulent air flow was carried out by Promvonge [22]. It was concluded that wire coils with a square cross-section are more capable of inducing turbulence in the flow, resulting in a greater enhancement of heat transfer compared to those with a circular cross-section. The friction factor, heat transfer rate and thermal enhancement efficiency were increased by the shorter pitch length.

Gunes et al. [23] figured out the effect of a wire coil having an equilateral triangular cross-section placed at a distance from the tube wall on the convective heat transfer rate and friction loss due to pressure drop in the turbulent regime of air flow. The study revealed that reducing the pitch length of the equilateral triangle resulted in higher pressure drop and enhanced heat transfer. Also, it was concluded that increasing the side length resulted in a proportional rise in both. Further, Gunes et al. [24] experimentally demonstrated the impact of distances from the tube at which equilateral triangular coiled wires were placed. The findings showed that a lower separation distance and coil pitch length yielded a superior overall enhancement ratio than the others. The influence of variation of the diameter of wires and lengths of pitch placed in a horizontal pipe was demonstrated by Akhavan-Behabadi et al. [25]. Improved thermal performance was noted in tubes using wire coils of smaller diameter. Additionally, it was found that low values of pitch lengths improve the heat transfer performance.

Chandrasekar et al. [26] determined the heat transfer rate and friction loss of a tubular heat exchanger using a combination of Al₂O₃-water nanofluid and wire coil inserts. The concentration of nanoparticles in the fluid was limited to 0.1% by volume. As the thermal conductivity of the working fluid was improved by the addition of Al₂O₃ nanoparticles, the combination of nanofluid with wire coils increased the Nusselt number by 15.91% and 21.53% at pitch ratios of 2 and 3, respectively. Additionally, the pressure drop associated with nanofluid was found to be almost equivalent to that of pure water. Eiamsa-ard et al. [27] reported the thermal characteristics heat exchanger having a square cross section with a tandem wire coil insert. Different insert lengths and free spacing configurations of wire coils were examined, and their performance was compared against that of a continuous, fulllength wire coil. It was found that the heat transfer improvement in a square duct using a continuous coil was greater than that achieved with tandem wire insertions. Saeedinia et al. [28] recommended a nanofluid containing CuO with a higher particle concentration along with conventional wire coil inserts to enhance the heat transfer rate in the laminar region. The heat transfer and fluid flow characteristics of a pipe inserted with wire coil inserts in the laminar and transitional flow conditions were reported by Martinez et al. [29]. Compared to a plain tube, the heat transfer rate showed an enhancement of up to 4.5 times, while the friction factor increased by approximately 3.5 times.

The experiments were conducted by Chang et al. [30] to identify the influence of square wire coils with grooved or ribbed structures having different pitch configurations on the heat transfer augmentation. According to their findings, the

modified square wire coils with grooves or ribs outperformed the smooth square wire coil in terms of performance factor across all pitch ratio variations. Syam Sundar et al. [31] analyzed the performance of a double pipe heat exchanger with U-bend by calculating values of the effectiveness and number of transfer units (NTU) in two scenarios- in the presence and absence of wire coil inserts with Fe₃O₄-water nanofluid. The results indicated that the NTU and effectiveness are directly proportional to the concentration of Fe₃O₄ particles. Both performance parameters were significantly reduced by the wire coils having a longer pitch. Du et al. [32] evaluated the thermo-hydraulic flow behavior in a corrugated tube containing modified wire coil inserts arranged at regular intervals. Results showed that the combination performed better than the standalone corrugated tube. Also, it was described that the increased friction caused by the introduction of coils resulted in a lower overall thermal performance.

Abdul Hamid et al. [33] investigated the influence of both pitch ratio and nanoparticle concentration on the heat transfer and flow characteristics of wire coil-inserted tubes using TiO2-SiO2 nanofluid. A pitch ratio of 1.5 for the wire coil and a 2.5% nanofluid volume concentration were found to be optimized performance affecting parameters. The effect of different wire coil orientations and spacing ratios on heat transfer in a transverse corrugated tube was experimentally studied by Hong et al. [34]. Findings of the study showed that a decrease in the spacing ratio significantly enhanced the convective heat transfer performance, along with a corresponding rise in the friction factor due to increased flow resistance. The effect of the circular, square and triangular cross-section of wire coil was evaluated by Yu et al. [35]. Due to the generation of strong turbulence compared to others, the square cross-section emerged as an efficient one. The average enhancement in heat transfer was found to be 26.25% for wire coils with a circular cross-section, 57.46% for those with a square cross-section, and 45.92% for coils with an equilateral triangular cross-section. Chompookham et al. [36] reported results obtained by introducing a serrated wire coil. A rise in Nusselt number was observed with a decrease in pitch length and an increase in coil diameter. But the friction factor showed a declining trend with larger coil diameter and extended pitch length. Within the tested range, the growth of 1.75–2.46 times and 3.31-8.16 times in Nu and f was observed.

The effect of combinations of helical wire coil-twisted tape [37, 38], rectangular wire coil-twisted tape [39] and wire coil-perforated conical ring [40] on the thermohydraulic performance of the heat exchanger was also reported in the literature. Although the combination resulted in enhanced thermal performance compared to the individual methods, it was accompanied by a comparatively higher pressure drop.

In-depth literature analysis indicates that incorporating helical wire coils improves convective heat transfer in heat exchangers, with considerable attention given to factors such as flow velocity, working fluid properties, pitch ratio, and coil geometry. The present study investigates the convective heat transfer and flow resistance behavior in a circular tube equipped with three variable diameter coils, namely convergent (C), divergent (D) and alternate convergent-divergent (CD) is investigated. The geometric parameters associated with these variable diameter coils are conical length ratio (CLR) and diameter ratio (DR) and CLR is defined as the ratio of conical length (L) to maximum diameter (D_m) of the coil, whereas DR is expressed as the ratio of wire diameter (d_w) to maximum coil diameter (D_m) . The geometry of a conical

element of variable diameter coil is represented in Figure 1. To maintain dimensional accuracy, 3D printing technology was used to manufacture the coils.

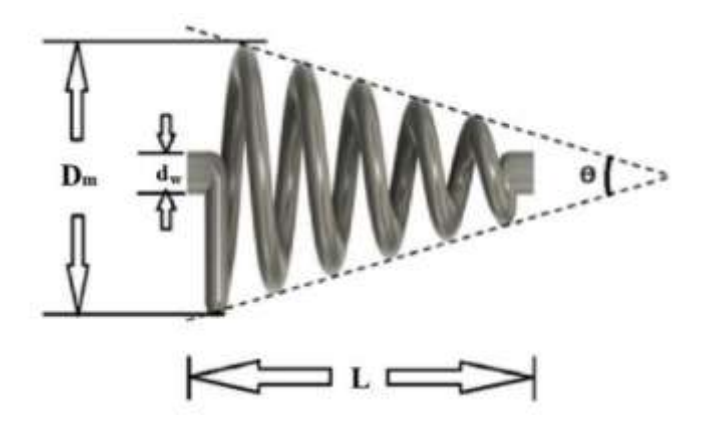


Figure 1. Geometry of a conical element of variable diameter helical coil

Previous investigations of conical passive enhancement techniques have primarily focused on the influence of pitch ratio and spacing length on heat transfer and pressure drop characteristics. However, the effect of the conical length ratio, which directly governs the slant height and apex angle of the conical element, on the thermo-hydraulic performance of tubular heat exchangers has not been reported in the literature, to the best of the authors' knowledge. So, in this study, efforts are taken to investigate the effect of CLR along with DR and Reynolds number (Re) on Nusselt number (Nu), friction factor (f) and thermal performance factor (TPF). Also, multicriterion optimization is carried out for each coil to determine the appropriate level of performance affecting parameters. The geometry of variable diameter helical coils is shown in Figure 2. The overall length of every coil used is 1000 mm, and the maximum diameter is 25 mm. Values of other geometric parameters associated with all three configurations of variable diameter helical coils are listed in Table 1.

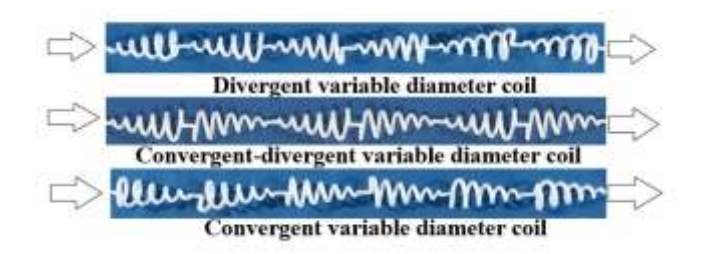


Figure 2. Actual geometries of variable diameter helical coils used in experimentation

Table 1. Values of geometric parameters of variable diameter helical coils

	Case-I	Case-II	Case-III
Conical length (L) in mm	50	75	100
Conical length ratio (CLR)	2	3	4
Wire diameter (d) in mm	3	4	5
Diameter ratio (DR)	0.12	0.16	0.2

2. DETAILS OF EXPERIMENTATION FACILITY AND PROCEDURE

A schematic layout of the experimentation facility is shown in Figure 3. A copper tube measuring 1000 mm in length, with an internal diameter of 26 mm and a wall thickness of 1 mm, was utilized as the test section. To ensure uniform heat input. an electric coil was spirally wound around the length of the test section. The electrical input was adjusted using a variac transformer. To minimize convective losses to the environment, the outer surface was insulated. Seven thermocouples were tapped on the outer wall of the tube to measure the temperature variation along the length of the tube. An orifice meter, designed as per ASME standards [41], was used to measure the volumetric flow rate of the water. A flow control valve was used to adjust the deflection of mercury across the orifice meter, which ultimately helped to set the desired value of Re. During experimentation, the Re was varied from 4000 to 10000. To accurately capture minor pressure fluctuations across the test length, a U-tube manometer filled with carbon tetrachloride was employed. For each test run, water from the reservoir was pumped through an orifice meter and subsequently into the test section. After attaining the steady state, surface temperatures of the tube, inlet and outlet temperatures of water and pressure drop across the test section were recorded. Properties of water required for calculations were considered at the mean bulk temperature.

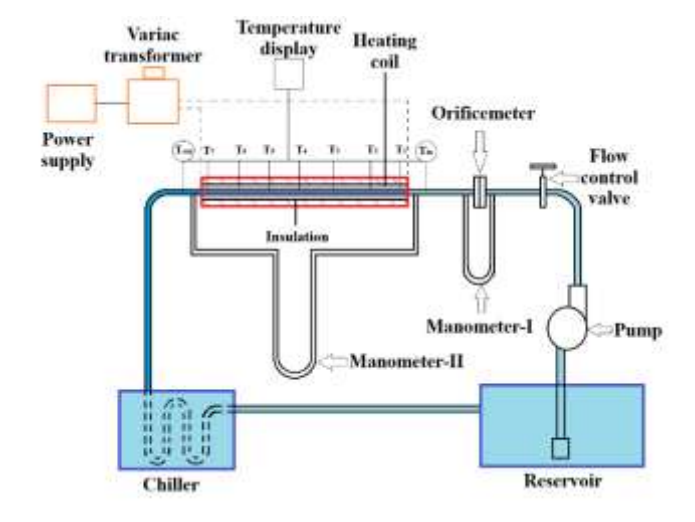


Figure 3. Schematic diagram of the experimental setup

3. DATA PROCESSING AND UNCERTAINTY ANALYSIS

Two key performance indicators, Nusselt number (Nu) and friction factor (f) are used to evaluate the efficacy of any heat transfer enhancement method. While the Nusselt number evaluates the rate of convective heat transfer, the friction factor indicates the associated pressure drop.

The rate of convective heat transfer is expressed by Eq. (1):

Heat convected =
$$Q_{conv.} = hA_s(T_s - T_b)$$
 (1)

where,

 $h = \text{Heat transfer coefficient in w/m}^2\text{K}$

 A_s = Surface area of the tube = π dl

d = Diameter of the tube in m

l =Length of the tube in m

 T_s = Mean surface temperature and it is given by Eq. (2):

$$T_{s} = \frac{T_{1} + T_{2} + T_{3} + T_{4} + T_{5} + T_{6} + T_{7}}{7} \tag{2}$$

 T_b = Mean bulk temperature, which is given by Eq. (3):

$$T_{b} = \frac{T_{in} + T_{out}}{2} \tag{3}$$

The heat transferred by the heating coil to the water is given by Eq. (4):

Heat absorbed by water = $Q_a = mC_p(T_{out} - T_{in})$ (4)

where

m = Mass flow rate of water in Kg/sec

 C_p = Specific heat of water at constant pressure

 T_{out} = Temperature of water at outlet

 T_{in} = Temperature of water at inlet

At steady state,

 $Q_a = Q_{conv.}$

So, the heat transfer coefficient is given by Eq. (5):

$$h = \frac{mC_p(T_{out} - T_{in})}{A_s(T_s - T_h)}$$
 (5)

Experimental Nusselt number (Nu) is given by Eq. (6):

$$Nu = \frac{hd}{k} \tag{6}$$

where, k = Thermal conductivity of water.

Experimental friction factor is calculated by Eq. (7):

$$f = \frac{\Delta p}{\frac{1}{d} \times \frac{\rho v^2}{2}} \tag{7}$$

where,

 Δp = Pressure drop in the test section in N/m²

 ρ = Density of water in Kg/m³

v =Velocity of water in m/sec

The thermal performance factor is calculated by Eq. (8):

$$TPF = \frac{\frac{N_{\rm u}}{N_{\rm u_o}}}{(\frac{f}{f_o})^{\frac{1}{3}}} \tag{8}$$

where, Nu and f are Nusselt number and friction factor for the tube equipped with coil inserts, while Nu_o and f_o represent the corresponding values for the plain tube.

The methodology for predicting the uncertainty of experimental results given by Kline and McClintock [42] is used. The method is effective in analyzing the errors arising in experimental work due to deviations in primary measurements. It determines the overall uncertainty of a derived quantity by combining the uncertainties of the individual primary measurements. The formulation is based on a first-order Taylor series expansion, which assumes small deviations in the measured variables. The distribution of error is assumed to be normal and the uncertainty in each variable (Y) is described as

$$Y = X \pm x$$

The above equation states that the best value of variable, Y is believed to be X and its true value lies within the interval (X + x, X - x).

The maximum uncertainties for dimensionless parameters Re, Nu, f and TPF are about \pm 2.01%, \pm 3.3%, \pm 2.94 and \pm 3.44% respectively. Eqs. (9)-(12) are used to determine the uncertainties.

$$\frac{\Delta Re}{Re} = \left[\left(\frac{\Delta m}{m} \right)^2 + \left(\frac{\Delta d}{d} \right)^2 \right]^{1/2} \tag{9}$$

$$\frac{\Delta Nu}{Nu} = \left[\left(\frac{\Delta h}{h} \right)^2 + \left(\frac{\Delta d}{d} \right)^2 \right]^{1/2} \tag{10}$$

$$\frac{\Delta f}{f} = \left[\left(\frac{\Delta d}{d} \right)^2 + \left(\frac{\Delta v}{v} \right)^2 + \left(\frac{\Delta l}{l} \right)^2 + \left(\frac{\Delta (\Delta p)}{\Delta p} \right)^2 \right]^{1/2} \tag{11}$$

$$\frac{\Delta TPF}{TPF} = \left[\left(\frac{\Delta Nu}{Nu} \right)^2 + \left(\frac{1}{3} \times \frac{\Delta f}{f} \right)^2 \right]^{1/2} \tag{12}$$

4. RESULTS AND DISCUSSION

4.1 Validation of experimental setup

The accuracy of the experimental setup was validated by comparing experimental values of Nusselt number and friction factor for a plain tube with those calculated using the Dittus-Boelter and Blasius correlations [43-45]. Figures 4 and 5 illustrate the results obtained. It can be concluded that the experimental values agree reasonably with the values obtained from correlations. The mean absolute percentage deviations are 3.42% and 3.01% for *Nu* and *f*, respectively.

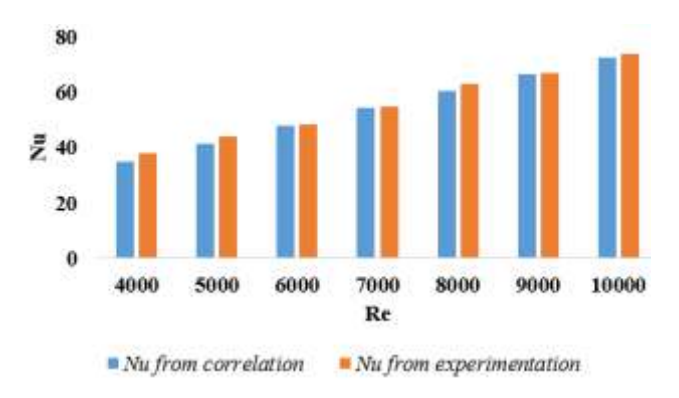


Figure 4. Validation of Nu for plain tube

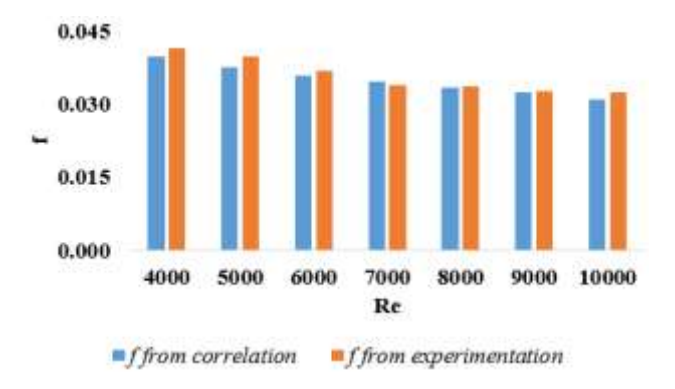


Figure 5. Validation of f for plain tube

Dittus-Boelter correlation is given by Eq. (13):

$$Nu = 0.023 \times Re^{0.8} \times Pr^{0.4} \tag{13}$$

Blassius correlation is given by Eq. (14):

$$f = \frac{0.3164}{Re^{0.25}} \tag{14}$$

where.

Re =Reynolds number and Pr =Prandtl number.

4.2 The influence of variable diameter helical coils on heat transfer rate and pressure drop

After carrying out validation of the experimental setup, the experiments were performed by introducing three configurations of variable diameter wire coils with three different *CLR* (2,3 and 4), three different *DR* (0.12, 0.16 and 0.2). The *Re* varied from 4000 to 10000 and water was used as a working fluid.

It has been revealed that the Nu is directly proportional to Re in each case. All configurations of variable diameter wire coils contribute to the rise in heat transfer rate compared to the plain tube. Figures 6, 7, and 8 illustrate the change in Nu with Re for all configurations of variable diameter helical coils at different DR. Within the tested range, the average increment in Nu compared to plain tube for convergent coils is 37.13%-74.17%, for convergent-divergent coils it is 47.18%-88.18% and for divergent coils it is 58.11%-100.79%. The increase in turbulent intensity is the main reason behind the improvement. The increased turbulent intensity results in better mixing in the flow field and it interrupts the formation of the boundary layer in which viscous effects are dominant. Also, the increase in the chaotic nature of the flow increases the residence time of fluid in the flow domain, facilitating extended heat exchange between the tube wall and the fluid.

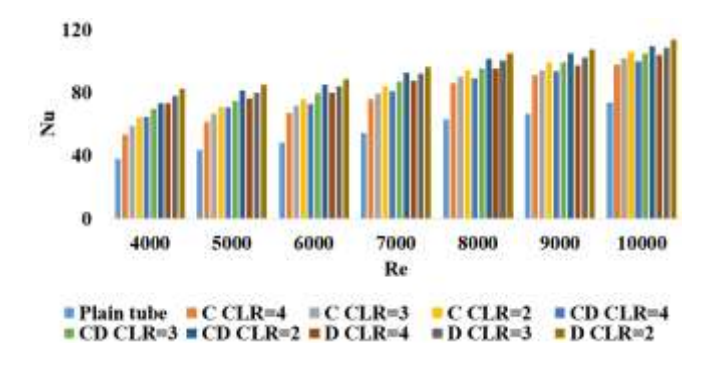


Figure 6. Variation of Nu with Re at DR = 0.12

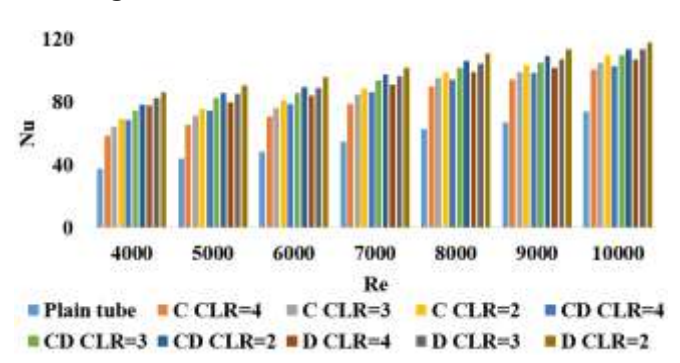


Figure 7. Variation of Nu with Re at DR = 0.16

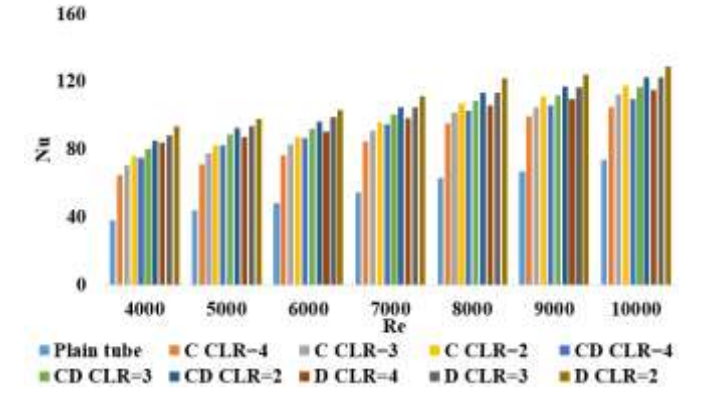


Figure 8. Variation of Nu with Re at DR = 0.2

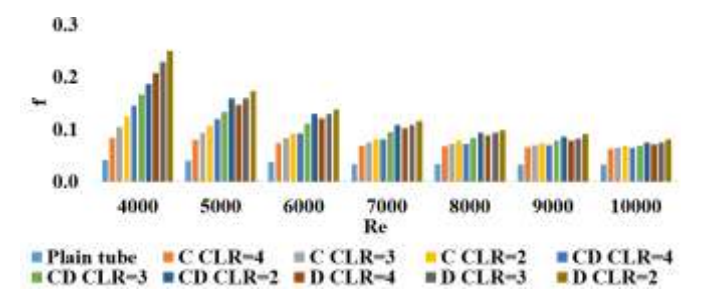


Figure 9. Variation of f with Re at DR = 0.12

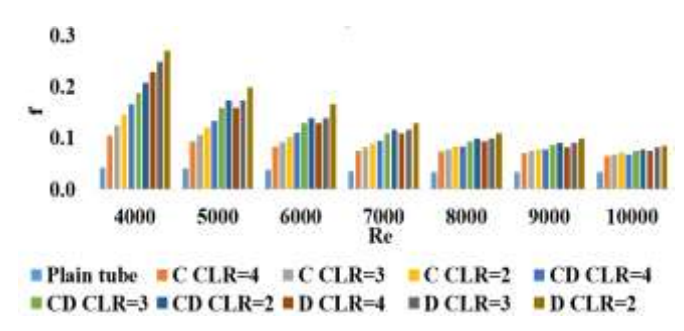


Figure 10. Variation of f with Re at DR = 0.16

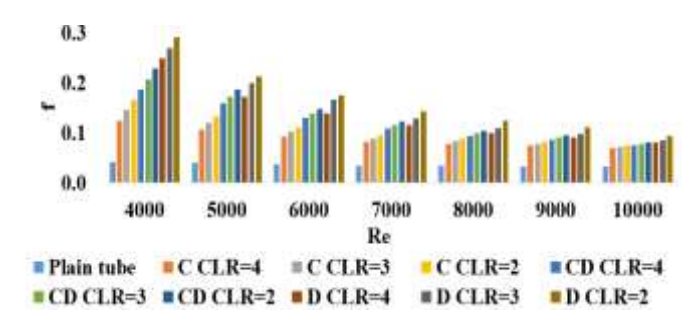


Figure 11. Variation of f with Re at DR = 0.2

It is seen from Figures 6, 7, and 8 that at the same CLR, DR and Re, the values of Nu are highest for the divergent variable diameter helical coils. The convergent-divergent coils show the relatively lower values of Nu and the convergent coils configuration shows the least values of Nu. The divergent variable diameter helical coils are efficient in moving the fluid from the core region of the flow to the peripheral region close to the wall. It destroys the boundary layer in which fluid experiences deceleration that ultimately increases turbulence intensity, thereby contributing a remarkable upswing in the heat transfer rate. For example, at the same DR = 0.12 and CLR = 4 average increment in Nu, in contrast to the plain tube, for

the divergent coil is 58.11%, for the convergent-divergent coil it is 47.18% and for the convergent coil it is 37.13%.

All three embedding types of variable diameter coils increase the pressure drop when introduced in the flow field. This results in an increase in the values of the friction factors. Figures 9, 10, and 11 depict the variation of f with Re for all configurations of variable diameter helical coils and different DR. Increase in value of f compared to plain tube for convergent coils is around 1.98-2.97 times, for convergentdivergent coils it is 2.55-3.8 times and for divergent coils it is 3.22-4.55 times. Divergent variable diameter coils show the highest values of f at the same CLR, DR and Re. The values of f for convergent-divergent coils are in between those of divergent and convergent coils. And convergent coils show the least values of f. Also, as expected, the value of f decreases with an increase in Re. For example, at DR = 0.12 and CLR =4 as compared to plain tube for divergent coil, f increases by 3.22 times, in case of convergent-divergent coil, it increases by 2.55 times and in case of convergent coil, it increases by 1.98 times.

4.3 Effect of conical length ratio

It is observed that for all three profiles of variable diameter coils, the lowest CLR results in high values of Nu. It is important to note that secondary flows are encouraged, and flow disturbance rises as the number of conical elements in the flow region increases because of lower CLR values. In the present study, three values of CLR = 2, 3, and 4 are considered. Compared with the empty tube at DR = 0.12, the average increment in Nu for convergent coils at CLR = 4 is 37.13%, at CLR = 3 it is 44.94% and at CLR = 2 it is 52.89%. In case of convergent-divergent coils, the improvement in Nu at CLR =4 is 47.18%, at CLR = 3 it is 57.14% and at CLR = 2 it is 66.95%. As earlier stated, divergent coils are most effective. For them, the average percentage augmentation in Nu over plain tube at CLR = 4 is 58.09%, at CLR = 3 it is 66.03% and at CLR = 2 it is 74.55%. At DR = 0.16 and for the same three CLRs, the average rise in Nu for convergent coils is observed as 43.81%, 53.44% and 61.26% respectively. For convergentdivergent coils, the values are 55.42%, 68.05% and 74.93% respectively. And for divergent coils, the values are 65.06%, 74.57% and 84.36% respectively. A similar trend is observed at DR = 0.2 also. At the same three CLRs, the average growth in Nu for convergent coils is seen as 53.51%, 64.84% and 74.19% respectively. The values of increments for convergentdivergent coils are 68.89%, 79.52% and 88.22% and for divergent coils, the values are 77.7%, 89.91% and 100.79% respectively.

Increased resistance to flow due to lower values of CLR results in higher values of f. Friction factor values are maximum at the lowest CLR for all three combinations at constant DR. Increased residence time of fluid in the test section due to more conical elements causes an upsurge in the pressure drop. In comparison with the plain tube at DR = 0.12, for convergent coils, f is increased by 1.98 times, 2.22 times and 2.47 times for CLR = 4, 3 and 2, respectively. Convergent-divergent coils show a hike in f by 2.55 times, 2.92 times and 3.33 times, whereas divergent coils show an increase in f by 3.22 times, 3.47 times and 3.75 times at the same CLRs. At DR = 0.16, the penalties of friction factor contrast to plain tube for convergent coils are 2.21 times, 2.45 times and 2.72 times, respectively. Results about convergent-divergent coils show growth of 2.91 times, 3.33 times and 3.55 times in f compared

to the plain tube. In the case of divergent coils, the values of rise in f are 3.47 times, 3.77 times and 4.19 times at the same CLRs. Similar patterns are also observed at DR = 0.2. For convergent coils, the increase in f is 2.47 times, 2.72 times and 2.97 times, respectively. In case of convergent-divergent coils, the values of rise in f are 3.33 times, 3.54 times and 3.8 times, respectively. The divergent coils exhibit the enhancement in f by 3.75 times, 4.2 times and 4.55 times within the tested range of CLRs.

4.4 Effect of diameter ratio (DR)

All three types of variable diameter coils show an increase in Nu with an increase in DR at the same CLR. The increase in DR is due to an increase in wire diameter, which results in increased obstruction to the flow. And it causes a rise in turbulent intensity, which enhances the heat transfer rate. At CLR = 4 for convergent coils average rise in Nu at DR = 0.12relative to plain tube is 37.15%, at DR = 0.16 it is 43.81% and at DR = 0.2 it is 53.48%. Similarly, for convergent-divergent coils the observed improvements in Nu are 47.18%, 55.41% and 68.86% respectively. In case of divergent coils, values of Nu are raised by 58.09%, 65.06% and 77.66% respectively for the same DRs. The resembling pattern is observed at CLR = 3and 2. At CLR = 3 and for the same DRs, convergent coils show a rise of 44.94%, 53.44% and 64.84% in Nu. Whereas convergent-divergent coils indicate the boost of 57.14%, 68.05% and 79.52% in Nu. Also, divergent coils show augmentation of 66.01%, 74.57% and 89.91% in Nu. At CLR = 2, increments of 52.89%, 61.26% and 74.15% in Nu are noticed for convergent coils. In case of convergent-divergent coils, the values of Nu are improved by 66.95%, 74.93% and 88.18%. For divergent coils, the increments of 74.55%, 84.36% and 100.79% are observed in values of Nu within the tested range of DRs.

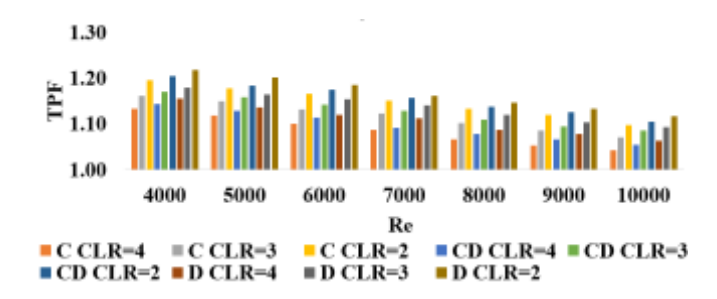


Figure 12. Variation of *TPF* with Re at DR = 0.12

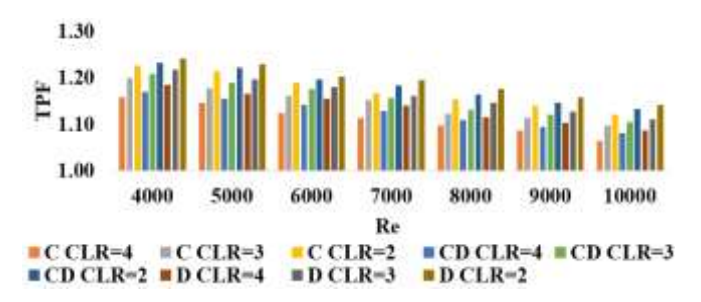


Figure 13. Variation of *TPF* with Re at DR = 0.16

4.5 Evaluation of thermal performance factor

Passive heat transfer enhancement techniques, while increasing the heat transfer rate, also lead to a higher pressure drop, which consequently results in an increased pumping

power requirement. Therefore, the thermal performance factor (TPF) is assessed to examine the usefulness of the employed technique. It is stated that the applied technique is beneficial if the TPF is greater than unity. In this study, TPF values for all three configurations at all CLR and DR are calculated. Variation of TPFs with Re at different DR is demonstrated in Figures 12, 13, and 14. It is observed that the values of TPF for all inserts are greater than unity, which highlights the promising nature of these variable diameter coils as a heat transfer augmentation technique. Also, as Re increases, TPF decreases. Highest values of TPF are observed at minimum values of CLR and maximum values of DR. Divergent variable diameter coils outperform when compared with their counterparts. For convergent coils, the highest and lowest values of TPF are 1.2694 and 1.0693, for convergentdivergent coils, they are 1.2807 and 1.073 and for divergent coils, the values are 1.2973 and 1.0842, respectively.

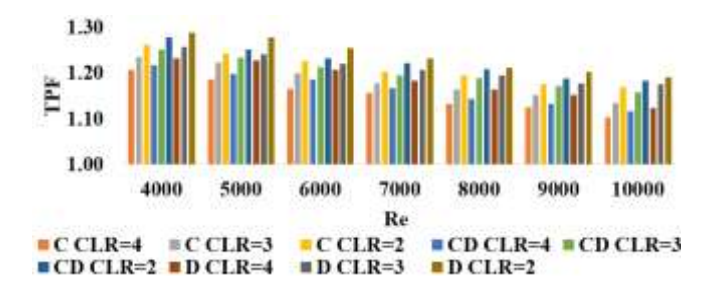


Figure 14. Variation of *TPF* with Re at DR = 0.2

The comparison of thermal performance factors (sometimes called enhancement efficiency) of various wire coil inserts is provided in Table 2.

Table 2. Maximum value of TPF for various wire coil inserts

Reference	Conditions	TPF
[46]	Wire coil having a triangular section positioned separately at a distance = 1 mm and having pitch ratio = 1 at $Re \approx 3430$	1.82
[36]	Serrated wire coils having the pitch ratio = 0.1969 and diameter ratio = 0.94 at $Re = 5114$.	1.41
[23]	Wire coil having triangular cross section with ratio of triangle length side to tube diameter = 0.0892 and pitch ratio = 1 at $Re \approx 3860$	1.37
This work	Divergent coil at $CLR = 2$, $DR = 0.2$ and ate $Re = 4000$	1.2973
This work	Convergent-divergent coil at $CLR = 2$, $DR = 0.2$ and ate $Re = 4000$	1.2807
This work	Convergent coil at $CLR = 2$, $DR = 0.2$ and ate $Re = 4000$	1.2694
[34]	Twin wire coils having a space ratio = 18.1 and Reynolds number around 9700 inserted in a traverse corrugated tube	1.09
[47]	Conventional wire coil having pitch ratio = 3 and at $Re = 4600$	1.01
[48]	The wire coil has changing pitch ratio ranging from 0.172 to 0.690 mm and Reynolds number close to 6200	0.99

5. RSM MODELLING

It is very challenging to conduct experiments for every

possible combination of input variables when a process is influenced by numerous variables. Design of experiments is a structured approach used to plan experiments so that appropriate data can be gathered and analyzed by statistical methods [49-51]. Response surface methodology (*RSM*) is a collection of quantitative methods designed to examine and model the relationship between multiple input variables and a desired output [52-54]. Also, it is typically used to understand how these factors interact and to determine optimal conditions for the best possible response. Hence, in the present analysis, *RSM* is applied to formulate predictive models for the Nusselt number (*Nu*) and friction factor (*f*), and to determine their optimal values under different fluid flow conditions and geometric parameters associated with variable diameter helical coils.

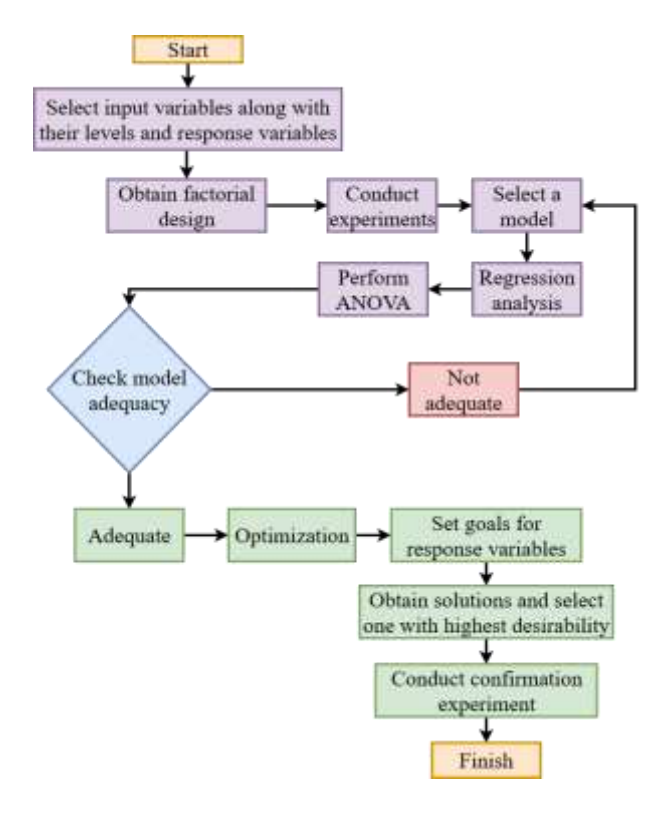


Figure 15. Flow chart for response surface methodology

RSM generally follows three essential steps. Initially, the significant independent variables and their respective levels are identified. Next, a mathematical model is developed to describe the relationship between these variables and the response, followed by validation of the model. Finally, contour and surface plots are generated to interpret the results and by applying constraints, the optimal operating conditions are obtained. The steps carried out in RSM analysis are described in Figure 15.

In the present study, *Re, CLR*, and *DR* are considered as input parameters and *Nu* and *f* are considered as response parameters. In the analysis, experimental data are gathered using the Central Composite Design (*CCD*). The factorial component of *CCD* includes a full factorial arrangement, covering every possible combination of the selected factors at two levels, high and low [55]. The design includes six axial points and six center points to adequately estimate the curvature of the response surface. The star points are located at the faces of the cube. This kind of configuration is called the face-centered *CCD* [56]. Commercially available Design Expert software was used for analysis. The arrangement

consists of 20 runs, and it is shown in Table 3. Values of Nu and f are taken from experimental results.

5.1 ANOVA analysis

To analyze the effects of the input variables, a polynomial regression approach is adopted. As a first-order (linear) model lacks the ability to capture the complex nature of the responses

effectively, a second-order (quadratic) model is used. The choice of quadratic models is justified by the observation that responses have been impacted by squared and interactive terms in addition to linear terms. Analysis of Variance (ANOVA) was conducted to determine the statistical significance of the parameters affecting the responses. Tables 4-9 show the ANOVA tables for responses Nu and f for three configurations of variable diameter coils.

Table 3. Matrix of experiments along with results

	CID	D.D.	Conver	gent Coils	Convergent-	Divergent Coils	Divergent Coils		
Re	CLR	DR	Nu	f	Nu	f	Nu	f	
4000	2	0.12	64	0.12	74	0.19	82	0.25	
10000	2	0.12	106	0.06	110	0.07	114	0.08	
4000	4	0.12	54	0.08	65	0.15	74	0.2	
10000	4	0.12	98	0.06	100	0.06	104	0.07	
4000	2	0.2	76	0.17	85	0.23	94	0.29	
10000	2	0.2	118	0.07	122	0.08	129	0.09	
4000	4	0.2	65	0.12	75	0.19	84	0.25	
10000	4	0.2	105	0.06	110	0.07	115	0.08	
4000	3	0.16	65	0.12	75	0.19	83	0.25	
10000	3	0.16	105	0.06	110	0.07	114	0.08	
7000	2	0.16	88	0.09	97	0.12	102	0.13	
7000	4	0.16	79	0.07	86	0.09	91	0.11	
7000	3	0.12	80	0.07	87	0.09	92	0.11	
7000	3	0.2	91	0.09	100	0.12	105	0.13	
7000	3	0.16	85	0.08	94	0.11	96	0.12	
7000	3	0.16	85	0.08	94	0.11	96	0.12	
7000	3	0.16	85	0.08	94	0.11	96	0.12	
7000	3	0.16	85	0.08	94	0.11	96	0.12	
7000	3	0.16	85	0.08	94	0.11	96	0.12	
7000	3	0.16	85	0.08	94	0.11	96	0.12	

Table 4. ANOVA table of Nu for convergent coils

			3.50			
Source	SS	df	MS	F-Value	p-Value	
Model	4936	9	548.45	1515.61	< 0.0001	significant
A-Re	4360	1	4359.74	12047.88	< 0.0001	
B-CLR	276.9	1	276.89	765.16	< 0.0001	
C-DR	286.6	1	286.55	791.85	< 0.0001	
AB	0.047	1	0.0465	0.1285	0.7274	
AC	2.28	1	2.28	6.3	0.0309	
BC	3.34	1	3.34	9.23	0.0125	
A^2	0.818	1	0.8182	2.26	0.1636	
B^2	0.7	1	0.7001	1.93	0.1944	
C^2	3.21	1	3.21	8.87	0.0138	
Residual	3.62	10	0.3619			
Lack of Fit	3.62	5	0.7237			
Pure Error	0	5	0			
Cor Total	4940	19				

Table 5. ANOVA table of f for convergent coils

Source	SS	df	MS	F-Value	p-Value	
Model	0.013	9	0.0014	175.38	< 0.0001	significant
A-Re	0.008	1	0.008	986.65	< 0.0001	
B-CLR	0.001	1	0.0012	150.12	< 0.0001	
C-DR	0.001	1	0.0012	150.12	< 0.0001	
AB	6E-04	1	0.0006	75.99	< 0.0001	
AC	6E-04	1	0.0006	75.99	< 0.0001	
BC	0	1	0	0	1	
A^2	6E-04	1	0.0006	76.77	< 0.0001	
B^2	0	1	0	0	1	
C^2	0	1	0	0	1	
Residual	1E-04	10	8.06E-06			
Lack of Fit	1E-04	5	0			
Pure Error	0	5	0			
Cor Total	0.013	19				

Table 6. ANOVA table of Nu for convergent-divergent coils

Source	SS	df	MS	F-Value	p-Value	
Model	3798	9	422	972.62	< 0.0001	significant
A-Re	3172	1	3171.96	7310.73	< 0.0001	
B-CLR	283.6	1	283.56	653.54	< 0.0001	
C-DR	330.7	1	330.74	762.29	< 0.0001	
AB	1.3	1	1.3	3.01	0.1136	
AC	0.113	1	0.1128	0.26	0.6212	
BC	2.13	1	2.13	4.91	0.051	
A^2	1.34	1	1.34	3.09	0.1093	
B^2	3.72	1	3.72	8.58	0.0151	
C^2	2.02	1	2.02	4.65	0.0564	
Residual	4.34	10	0.4339			
Lack of Fit	4.34	5	0.8678			
Pure Error	0	5	0			
Cor Total	3802	19				

Table 7. ANOVA table of f for convergent-divergent coils

Source	SS	df	MS	F-Value	p-Value	
Model	0.039	9	0.0043	1344.75	< 0.0001	significant
A-Re	0.032	1	0.032	10008.99	< 0.0001	
B-CLR	0.001	1	0.0014	442.44	< 0.0001	
C-DR	0.001	1	0.0014	442.44	< 0.0001	
AB	6E-04	1	0.0006	175.31	< 0.0001	
AC	6E-04	1	0.0006	175.31	< 0.0001	
BC	1.13E-06	1	1.13E-06	0.3515	0.5664	
A^2	0.002	1	0.0017	517.65	< 0.0001	
B^2	2.51E-06	1	2.51E-06	0.7829	0.397	
C^2	2.51E-06	1	2.51E-06	0.7829	0.397	
Residual	0	10	3.20E-06			
Lack of Fit	0	5	6.40E-06			
Pure Error	0	5	0			
Cor Total	0.039	19				

Table 8. ANOVA table of Nu for divergent coils

Source	SS	df	MS	F-Value	p-Value	
Model	3207	9	356.35	1744.96	< 0.0001	significant
A-Re	2523	1	2523.33	12356.31	< 0.0001	
B-CLR	273.8	1	273.84	1340.96	< 0.0001	
C-DR	367.6	1	367.6	1800.07	< 0.0001	
AB	3.1	1	3.1	15.18	0.003	
AC	2.58	1	2.58	12.62	0.0053	
BC	2.95	1	2.95	14.46	0.0035	
A^2	5.21	1	5.21	25.53	0.0005	
B^2	0.305	1	0.3053	1.49	0.2495	
C^2	8.49	1	8.49	41.56	< 0.0001	
Residual	2.04	10	0.2042			
Lack of Fit	2.04	5	0.4084			
Pure Error	0	5	0			
Cor Total	3209	19				

Table 9. ANOVA table of f for divergent coils

Source	SS	df	MS	F-Value	p-Value	
Model	0.0859	9	0.0095	2054.15	< 0.0001	significant
A-Re	0.0699	1	0.0699	15035.9	< 0.0001	
B-CLR	0.0016	1	0.0016	347	< 0.0001	
C-DR	0.0016	1	0.0016	347	< 0.0001	
AB	0.0005	1	0.0005	96.81	< 0.0001	
AC	0.0005	1	0.0005	96.81	< 0.0001	
BC	5.00E-07	1	5.00E-07	0.1076	0.7497	
A^2	0.0062	1	0.0062	1337.42	< 0.0001	
B^2	3.01E-06	1	3.01E-06	0.6466	0.44	
C^2	3.01E-06	1	3.01E-06	0.6466	0.44	
Residual	0	10	4.65E-06			
Lack of Fit	0	5	9.30E-06			
Pure Error	0	5	0			
Cor Total	0.086	19				

The quadratic model is used to develop the relationship between input and response variables. The equations for response variables consist of linear, interaction and squared terms and are given by Eqs. (15)-(20).

For convergent coils,

$$Nu = +33.61496 + 0.006747 \times Re + 0.172356 \times CLR - 2.66174 \times DR + 0.000025 \times Re \times CLR - 0.004448Re \times DR - 16.15625 \times CLR \times DR + 6.06061exp - 08 \times Re^2 - 0.504545 \times CLR^2 + 675.28409 \times DR^2$$
(15)

$$f = +0.197050 - 0.000030 \times Re - 0.031417 \times CLR + 0.785417 \times DR + 2.91667exp - 06 \times Re \times CLR - 0.000073 \times Re \times DR - 1.14174exp - 15CLR \times DR + 1.66667E - 09 \times Re^2 - 2.64742exp - 17 \times CLR^2 - 7.19178exp - 15 \times DR^2$$

$$(16)$$

For convergent-divergent coils,

$$\begin{aligned} Nu &= +36.31393 + 0.007268 \times Re + 4.66117 \times \\ CLR &+ 4.20303 \times DR - 0.000135 \times Re \times CLR + \\ 0.000990 \times Re \times DR - 12.90625 \times CLR \times DR - \\ 7.75758exp &- 08Re^2 - 1.16318 \times CLR^2 + \\ &- 535.51136 \times DR^2 \end{aligned} \tag{17}$$

$$f = +0.322080 - 0.000054 \times Re - 0.027214 \times CLR + 0.948826 \times DR + 2.79167exp - 06 \times Re \times CLR - 0.000070 \times Re \times DR + 0.009375 \times CLR \times DR + 2.72727exp - 09 \times Re^2 - 0.000955 \times CLR^2 - 0.596591 \times DR^2$$

$$(18)$$

For divergent coils,

$$Nu = +77.20890 + 0.003019 \times Re + 0.648591 \times CLR - 187.33030 \times DR - 0.000207 \times Re \times CLR + 0.004729 \times Re \times DR - 15.18750 \times CLR \times (19)$$

$$DR + 1.52980exp - 07 \times Re^{2} - 0.333182 \times CLR^{2} + 1098.01136 \times DR^{2}$$

$$f = +0.562843 - 0.000099 \times Re - 0.035473 \times CLR + 0.564659 \times DR + 2.50000exp - 06 \times Re \times CLR - 0.000062 \times Re \times DR - 0.006250 \times CLR \times DR + 5.28283exp - 09 \times Re^2 + 0.001045 \times CLR^2 + 0.653409 \times DR^2$$
 (20)

After several refinement cycles, the most suitable models were identified and their performance was assessed by calculating values of coefficients of determination (R^2) to ensure satisfactory predictive accuracy. It is calculated by Eq. (21).

$$R^2 = 1 - \frac{Residual}{CorTotal} \tag{21}$$

The model design fit statistics show values of (R^2) as 0.9993 and 0.9937 for Nu and f, respectively, in the case of convergent coils. For convergent-divergent coils, the values are 0.9989 and 0.9992, respectively and for divergent coils, the values are 0.9994 and 0.9995, respectively. R^2 value suggests the extent to which the model accurately captures the interconnection between independent and response variables, making it reliable for prediction and optimization [57, 58]. Adjusted R^2

and predicted R^2 are also determined by Eq. (22) and Eq. (23), respectively.

$$Adjusted R^{2} = 1 -$$

$$Residual/Residual df$$

$$Residual+ModelSS)/(Residualdf+modeldf)$$
(22)

Predicted
$$R^2 = 1 - \frac{Predicted\ error\ sum\ of\ squares}{Residual + Model\ SS}$$
 (23)

The adjusted R^2 and predicted R^2 values are summarized in Table 10.

Table 10. Values of adjusted R^2 and predicted R^2

Model	Adjusted R ²	Predicted R ²
Nu for convergent coils	0.9986	0.9904
f for convergent coils	0.988	0.9505
Nu for convergent-divergent coils	0.9978	0.9926
f for convergent-divergent coils	0.9984	0.9948
Nu for divergent coils	0.9988	0.9893
f for divergent coils	0.999	0.9963

Adjusted R^2 is a revised version of R^2 that penalizes the inclusion of irrelevant variables. Predicted R^2 helps to assess the predictive ability of a regression model for new, unseen data

The significant terms affecting the responses are decided based on *p*-value of the *ANOVA* table. If *p*-value is greater than 0.1, then those model terms are not significant. For convergent variable diameter coils for determination of values of Nu. all linear terms Re. CLR. DR. interaction terms Re \times DR and CLR $\times DR$ and the squared term DR^2 are significant model terms. Whereas for the determination of f, all linear terms Re, CLR, DR, interaction terms $Re \times CLR$ and $Re \times DR$ and one squared term Re^2 are significant. In case of the convergent-divergent variable diameter coils for determination of Nu the significant terms are Re, CLR, DR, CLR \times DR, CLR² and DR². For determination of f the significant terms are Re, CLR, DR, Re \times CLR and $Re \times DR$ and Re^2 . For the third configuration, i.e. in case of divergent variable diameter wire coils for the prediction of Nu, the significant terms are Re, CLR, DR, Re \times *CLR*, $Re \times DR$, $CLR \times DR$, Re^2 and DR^2 . The significant terms to predict values of f are Re, CLR, DR, Re \times CLR and Re \times DR and Re^2 .

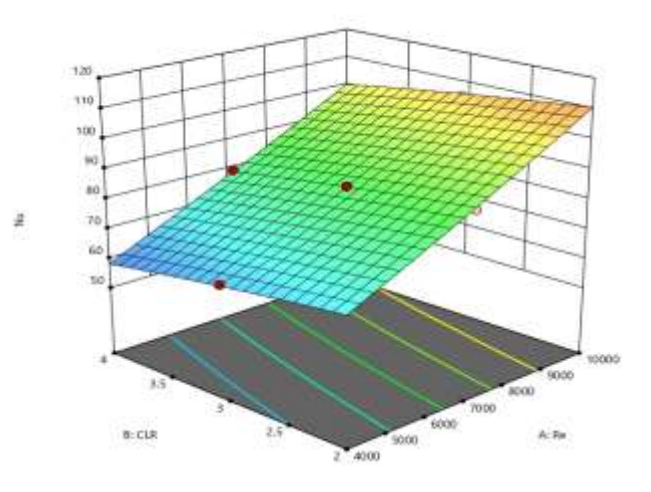


Figure 16. Combined effect of Re and CLR on Nu

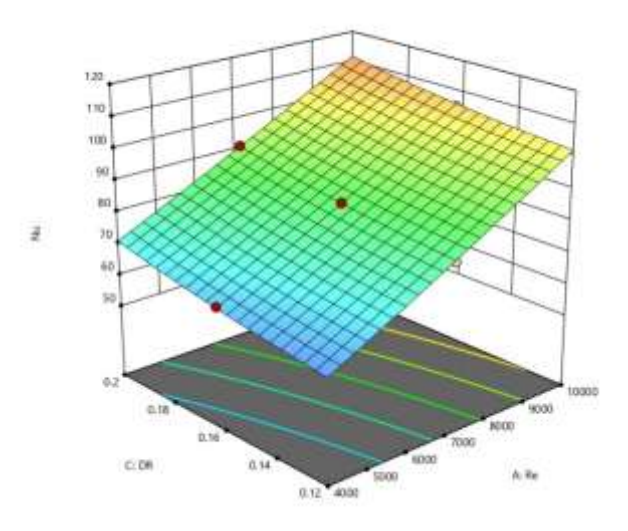


Figure 17. Combined effect of Re and DR on Nu

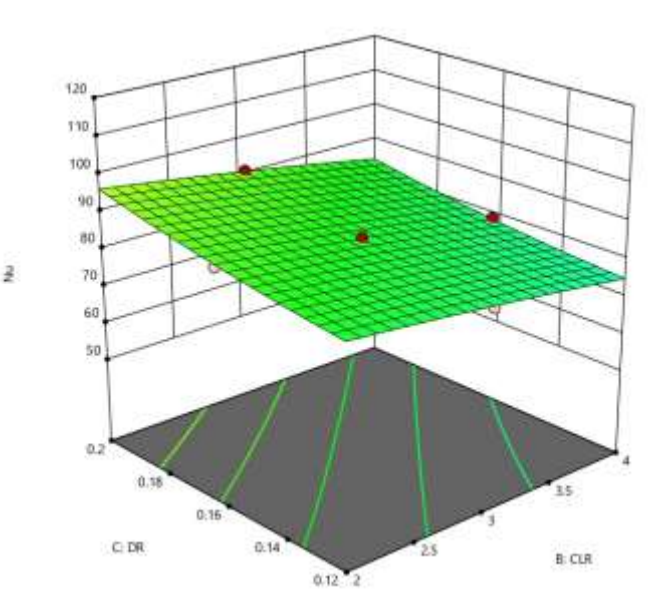


Figure 18. Combined effect of CLR and DR on Nu

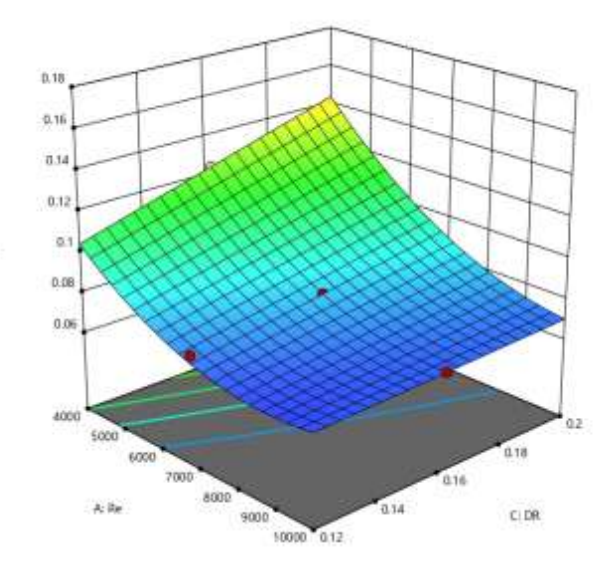


Figure 19. Combined effect of *Re* and *CLR* on *f*

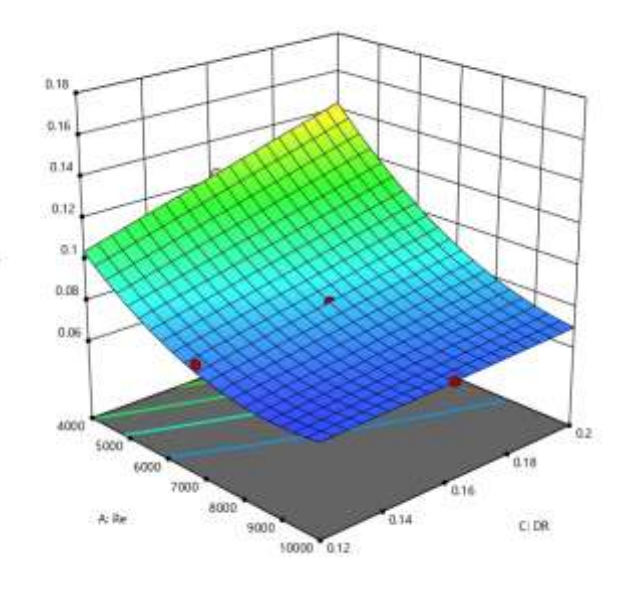


Figure 20. Combined effect of Re and DR on f

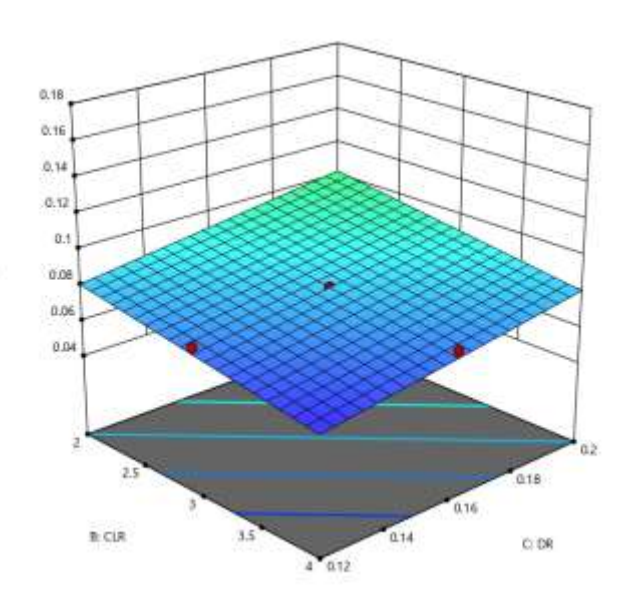


Figure 21. Combined effect of CLR and DR on f

The 3D surface plots obtained from RSM analysis provide insights into the variation of response variables with respect to the input variables. With 3D plots, it becomes easy to understand the combined effect of factors on the response variable. 3D surface plots for Nu for all three configurations of variable diameter helical coils are shown in Figures 16, 17, and 18. Higher values of Re and DR and lower values of CLR promote turbulence inside the flow field and hence result in higher values of Nu. 3D surface plots for f for all three configurations of variable diameter helical coils are shown in Figures 19, 20, and 21. As far as f is concerned, lower values of Re and CLR and higher values of DR increase resistance to flow and hence higher values of f are observed in these conditions.

5.2 Optimization

The primary objective of any heat transfer enhancement method is to attain higher values of Nu with minimal increases in the f. For optimization, the desirability function approach is

employed with the objective of maximizing Nu and minimizing f. Every response is transformed into a corresponding desirability value (D). It evaluates the degree to which the set of input variables meets the objective specified for the chosen response. The value of desirability ranges from 0 to 1. A desirability value of 1 indicates that the selected set of input factors perfectly meets the optimization objectives decided for the responses. Desirability functions for maximizing and minimizing the goals by using RSM [59] are given by Eq. (24) and Eq. (25).

$$D_{i} = \begin{cases} 0 & If PR < LV \\ \left(\frac{PR - LV}{TV - LV}\right)^{r} & LV < PR < TV \\ 1 & PR > TV \end{cases}$$
 (24)

$$D_{i} = \begin{cases} \frac{1}{\left(\frac{PR - UV}{TV - UV}\right)^{r}} & If \ PR < TV \\ \frac{PR - UV}{TV - UV} & TV < PR < UV \end{cases}$$

$$(25)$$

where, PR represents predicted values, LV denotes the minimum response value observed across all cases, UV indicates the maximum response value observed, TV refers to the desired or target value of the response and r is a weighting factor that reflects the relative importance of the response. The combination of input variables with the highest desirability is chosen as the optimum input variables. The optimal operating conditions are identified at the highest Re, the lowest CLR, and the maximum DR. The values of optimum input variables for Re, CLR, and DR are 10000, 2, and 0.2, respectively. The results of optimization are shown in Figure 22. Optimized values of Nu and f, along with the value of desirability for all three categories of variable diameter helical coils, are given in Table 11.

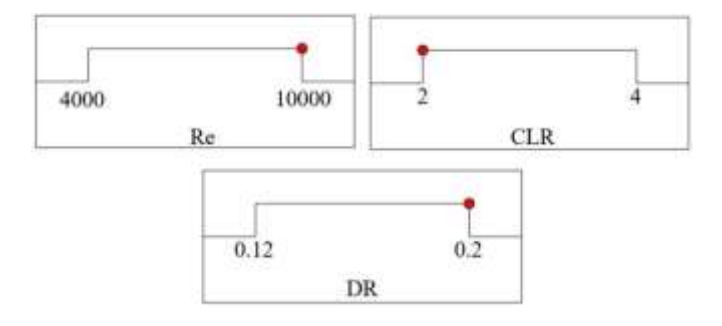


Figure 22. Optimum levels of input variables

Table 11. Results of optimization

	Optimized Response	Desirability	
	Nu	f	
Divergent variable diameter helical coils	128.35	0.0926	0.946
Convergent-divergent variable diameter helical coils	122.21	0.0798	0.953
Convergent variable diameter helical coils	117.1	0.0723	0.94

5.3 Confirmation experiment

To ensure the reliability of the proposed model, confirmation tests are carried out for each category of variable diameter helical coil. The confirmation experiments were performed at Re = 7000, CLR = 3, and DR = 0.16. The results obtained are shown in Table 12. Corresponding values of response variables predicted by models are also mentioned in Table 12. The average deviation for Nu is found to be 0.2596%, and for f, it is 1.91%. These values are significantly lower than the typical uncertainty margins encountered in experimental heat transfer research, which highlights the reliability of the present model. The close agreement between prediction and observation demonstrates that the RSM-based equations successfully capture the combined effects of input variables. Furthermore, the minimal discrepancies confirm that no major systematic errors are present in the modeling framework. This high level of consistency not only increases confidence in the model's predictive capability but also suggests its suitability for practical applications where accurate estimation of Nu and f is essential. This confirms that the response equations developed using RSM are reliable for predicting Nu and f across the range of input parameters studied.

Table 12. Results of confirmation experiments

	Convergent Coils		Dive	Convergent Divergent Coils		Divergent Coils	
	Nu	f	Nu	f	Nu	f	
Value predicted by model	84.39	0.079	93.36	0.109	96.72	0.118	
Experimental result	84.58	0.081	93.65	0.108	96.48	0.115	
Percentage variation	0.21	1.79	0.31	0.64	0.25	3.30	

6. CONCLUSIONS AND FUTURE SCOPE

An experimental investigation is carried out to analyze the thermo-hydraulic performance of a circular tube equipped with three configurations of variable diameter wire coils, namely convergent, convergent-divergent and divergent. The effect of conical length ratio, diameter ratio and Reynolds number on Nusselt number, friction factor and thermal performance factor is demonstrated. The analysis is followed by multicriteria optimization by using *RSM*. The important conclusions of the study are as follows:

- All three coil configurations significantly enhance heat transfer compared to a plain tube, with *TPF* values exceeding unity across the tested range. Maximum and minimum *TPF* values were 1.2694– 1.0693 for convergent coils, 1.2807–1.073 for convergent–divergent coils, and 1.2973–1.0842 for divergent coils.
- 2. Divergent variable diameter coils are more efficient than convergent and convergent-divergent variable diameter coils.
- Introduction of variable diameter helical coils in the flow field also results in an enhancement in friction loss.
- 4. It is observed that the increase in *DR* and decrease in *CLR* result in an increase in *Nu* and *f*.
- 5. As the values of the coefficient of determination for all cases are greater than 0.99, it can be concluded that the quadratic model formulated using RSM effectively captures the relationship between input

- parameters and response variables.
- 6. Optimized conditions to maximize Nu and minimize f are CLR = 2, DR = 0.2, and Re = 10000.

This study demonstrates that variable-diameter helical coils offer a practical and effective method to enhance heat transfer in tubular heat exchangers, providing design guidance for industrial applications where improved thermal performance and energy efficiency are critical.

While this study demonstrates the effectiveness of variablediameter helical coils in enhancing thermal performance, future work could explore their integration with other heat transfer enhancement techniques, as well as their application in non-circular ducts, multi-phase flows, and low-Reynoldsnumber regimes to broaden practical applicability.

REFERENCES

- [1] Alam, T., Kim, M. (2018). A comprehensive review on single phase heat transfer enhancement techniques in heat exchanger applications. Renewable and Sustainable Energy Reviews, 81: 813-839. https://doi.org/10.1016/j.rser.2017.08.060
- [2] Kirkar, S., Gonul, A., Celen, A., Dalkilic, A. (2023). Multi-objective optimization of single-phase flow heat transfer characteristics in corrugated tubes. International Journal of Thermal Sciences, 186: 108119. https://doi.org/10.1016/j.ijthermalsci.2022.108119
- [3] Sun, C., Wang, W., Tian, X., Suo, W., Qian, S., Bao, H. (2025). Optimizing heat transfer enhancement in helical tube with twisted tape using NSGA-II for multi-objective design. International Journal of Thermal Sciences, 210: 109630.
 - https://doi.org/10.1016/j.ijthermalsci.2024.109630
- [4] Rashidi, S., Eskandarian, M., Mahian, O., Poncet, S. (2019). Combination of nanofluid and inserts for heat transfer enhancement, Journal of Thermal Analysis and Calorimetry, 135: 437-460. https://doi.org/10.1007/s10973-018-7070-9
- [5] Farhadi, S., Shekari, Y., Omidvar, P. (2024). Numerical and experimental investigation of laminar and turbulent convective heat transfer in a coiled flow reverser with twisted tape insert. International Journal of Thermal Sciences, 197: 108781. https://doi.org/10.1016/j.ijthermalsci.2023.108781
- [6] Liu, S., Sakr, M. (2013). A comprehensive review on passive heat transfer enhancements in pipe exchangers. Renewable and Sustainable Energy Reviews, 19: 64-81. https://doi.org/10.1016/j.rser.2012.11.021
- [7] Sheikholeslami, M., Gorji-Bandpy, M., Ganji, D.D. (2015). Review of heat transfer enhancement methods: Focus on passive methods using swirl flow devices. Renewable and Sustainable Energy Reviews, 49: 444-469. https://doi.org/10.1016/j.rser.2015.04.113
- [8] Mousa, M.H., Miljkovic, N., Nawaz, K. (2021). Review of heat transfer enhancement techniques for single phase flows. Renewable and Sustainable Energy Reviews, 137: 110566. https://doi.org/10.1016/j.rser.2020.110566
- [9] Deshmukh, V., Sarviya, R.M. (2024). Categorical review of experimental and numerical studies on twist tape inserts in the single-phase flow tubular heat exchanger. Journal of Thermal Analysis and Calorimetry, 149: 2985-3025. https://doi.org/10.1007/s10973-024-12886-2

- [10] He, J., Deng, Q., Feng, Z. (2022). Heat transfer enhancement of impingement cooling with corrugated target surface. International Journal of Thermal Sciences, 171: 107251. https://doi.org/10.1016/j.ijthermalsci.2021.107251
- [11] Rashidi, S., Mahian, O., Languri, E.M. (2018). Applications of nanofluids in condensing and evaporating systems. Journal of Thermal Analysis and Calorimetry, 131: 2027-2039. https://doi.org/10.1007/s10973-017-6773-7
- [12] Amirahmadi, S., Rashidi, S., Abolfazli Esfahani, J. (2016). Minimization of exergy losses in a trapezoidal duct with turbulator, roughness and beveled corners. Applied Thermal Engineering, 107: 533-543. https://doi.org/10.1016/j.applthermaleng.2016.06.182
- [13] Kareem, Z.S., Mohd Jaafar, M.N., Lazim, T.M., Abdullah, S., Abdulwahid, A.F. (2015). Passive heat transfer enhancement review in corrugation. Experimental Thermal and Fluid Science, 68: 22-38. https://doi.org/10.1016/j.expthermflusci.2015.04.012
- [14] Zhang, J.N., Cheng, M., Ding, Y.D., Fu, Q., Chen, Z.Y. (2019). Influence of geometric parameters on the gas-side heat transfer and pressure drop characteristics of three-dimensional finned tube. International Journal of Heat and Mass Transfer, 133: 192-202. https://doi.org/10.1016/j.ijheatmasstransfer.2018.12.118
- [15] Hajmohammadi, M.R., Doustahadi, A., Ahmadian-Elmi, M. (2020). Heat transfer enhancement by a circumferentially non-uniform array of longitudinal fins assembled inside a circular channel. International Journal of Heat and Mass Transfer, 158: 120020. https://doi.org/10.1016/j.ijheatmasstransfer.2020.12002
- [16] Liu, L., Cao, Z., Shen, T., Zhang, L., Zhang, L. (2021). Experimental and numerical investigation on flow and heat transfer characteristics of a multi-waves internally spiral finned tube. International Journal of Heat and Mass Transfer, 172: 121104. https://doi.org/10.1016/j.ijheatmasstransfer.2021.12110
- [17] Maleki, N.M., Pourahmad, S. (2023). Heat transfer enhancement in a heated copper tube using the electromagnetic vibration method for nanofluids as working fluid: An experimental study. International Communications in Heat and Mass Transfer, 141: 106566. https://doi.org/10.1016/j.icheatmasstransfer.2022.10656
- [18] Leal, L., Miscevic, M., Lavieille, P., Amokrane, M., Pigache, F., Topin, F., Nogarede, B., Tadrist, L. (2013). An overview of heat transfer enhancement methods and new perspectives: Focus on active methods using electroactive materials. International Journal of Heat Mass Transfer, 61: 505-524. https://doi.org/10.1016/j.ijheatmasstransfer.2013.01.083
- [19] Almahmmadi, B.A., Refaey, H.A., Abdelghany, M.T., Bendoukha, S., Mansour, M., Sharafeldin, M.A. (2024). Thermo-fluid performance for helical coils inserted in a tube using hybrid CFD-ANN approach. Thermal Science and Engineering Progress, 51: 102661. https://doi.org/10.1016/j.tsep.2024.102661
- [20] Garcia, A., Vicente, P.G., Viedma, A. (2005). Experimental study of heat transfer enhancement with wire coil inserts in laminar-transition-turbulent regimes

- at different Prandtl numbers. International Journal of Heat Mass Transfer, 48: 4640-4651. https://doi.org/10.1016/j.ijheatmasstransfer.2005.04.024
- [21] Naphon, P. (2006). Effect of coil—wire insert on heat transfer enhancement and pressure drop of the horizontal concentric tubes. International Communications in Heat and Mass Transfer, 33: 753-763. https://doi.org/10.1016/j.icheatmasstransfer.2006.01.02 0
- [22] Promvonge, P. (2008). Thermal performance in circular tube fitted with coiled square wires. Energy Conversion and Management, 49: 980-987. https://doi.org/10.1016/j.enconman.2007.10.005
- [23] Gunes, S., Ozceyhan, V., Buyukalaca, O. (2010). Heat transfer enhancement in a tube with equilateral triangle cross sectioned coiled wire inserts. Experimental Thermal and Fluid Science, 34: 684-691. https://doi.org/10.1016/j.expthermflusci.2009.12.010
- [24] Gunes, S., Ozceyhan, V., Buyukalaca, O. (2010). The experimental investigation of heat transfer and pressure drop in a tube with coiled wire inserts placed separately from the tube wall. Applied Thermal Engineering, 30: 1719-1725.
- https://doi.org/10.1016/j.applthermaleng.2010.04.001
 [25] Akhavan-Behabadi, M.A., Kumar, R., Salimpour, M.R., Azimi, R. (2010). Pressure drop and heat transfer augmentation due to coiled wire inserts during laminar flow of oil inside a horizontal tube. International Journal of Thermal Sciences, 49: 373-379. https://doi.org/10.1016/j.ijthermalsci.2009.06.004
- [26] Chandrasekar, M., Suresh, S., Chandra Bose, A. (2010). Experimental studies on heat transfer and friction factor characteristics of Al₂O₃/water nanofluid in a circular pipe under laminar flow with wire coil inserts. Experimental Thermal and Fluid Science, 34: 122-130. https://doi.org/10.1016/j.expthermflusci.2009.10.001
- [27] Eiamsa-ard Smith, N., Koolnapadol, N., Promvonge, P. (2012). Heat transfer behavior in a square duct with tandem wire coil element insert. Chinese Journal of Chemical Engineering, 20(5): 863-869. https://doi.org/10.1016/S1004-9541(12)60411-X
- [28] Saeedinia, M., Akhavan-Behabadi, M.A., Nasr, M. (2012). Experimental study on heat transfer and pressure drop of nanofluid flow in a horizontal coiled wire inserted tube under constant heat flux. Experimental Thermal and Fluid Science, 36: 158-168. https://doi.org/10.1016/j.expthermflusci.2011.09.009
- [29] Martinez, D.S., Garcia, A., Solano, J.P., Viedma, A. (2014). Heat transfer enhancement of laminar and transitional Newtonian and non-Newtonian flows in tubes with wire coil inserts. International Journal of Heat Mass Transfer, 76: 540-548. https://doi.org/10.1016/j.ijheatmasstransfer.2014.04.060
- [30] Chang, S.W., Gao, J.Y., Shih, H.L. (2015). Thermal performances of turbulent tubular flows enhanced by ribbed and grooved wire coils. International Journal of Heat Mass Transfer, 90: 1109-1124. https://doi.org/10.1016/j.ijheatmasstransfer.2015.07.070
- [31] Syam Sundar, L., Bhramara, P., Ravi Kumar, N.T., Singh, M.K., Sousa, A.C.M. (2017). Experimental heat transfer, friction factor and effectiveness analysis of Fe₃O₄ nanofluid flow in a horizontal plain tube with return bend and wire coil inserts. International Journal of Heat Mass Transfer, 109: 440-453.

- https://doi.org/10.1016/j.ijheatmasstransfer.2017.02.022
- [32] Du, J., Hong, Y., Wang, S., Ye, W.B., Huang, S.M. (2018). Experimental thermal and flow characteristics in a traverse corrugated tube fitted with regularly spaced modified wire coils. International Journal of Thermal Sciences, 133: 330-340. https://doi.org/10.1016/j.iithermalsci.2018.05.032
- [33] Abdul Hamid, K., Azmi, W.H., Mamat, R., Sharma, K.V. (2019). Heat transfer performance of TiO₂–SiO₂ nanofluids in a tube with wire coil inserts. Applied Thermal Engineering, 152: 275-286. https://doi.org/10.1016/j.applthermaleng.2019.02.083
- [34] Hong, Y., Du, J., Wang, S., Ye, W.B., Huang, S.M. (2019). Turbulent thermal–hydraulic and thermodynamic characteristics in a traverse corrugated tube fitted with twin and triple wire coils. International Journal of Heat Mass Transfer, 130: 483-495. https://doi.org/10.1016/j.ijheatmasstransfer.2018.10.087
- [35] Yu, C., Zhang, H., Wang, Y., Zeng, M., Gao, B. (2020). Numerical study on turbulent heat transfer performance of twisted oval tube with different cross sectioned wire coil. Case Studies in Thermal Engineering, 22: 100759. https://doi.org/10.1016/j.csite.2020.100759
- [36] Chompookham, T., Chingtuaythong, W., Chokphoemphun, S. (2022). Influence of a novel serrated wire coil insert on thermal characteristics and air flow behavior in a tubular heat exchanger. International Journal of Thermal Sciences, 171: 107184. https://doi.org/10.1016/j.ijthermalsci.2021.107184
- [37] Ravikiran, B., Ramji, K., Subrahmanyam, T. (2021). Investigation on thermal performance of different wire coil twisted tape inserts in a tube circulated with water. International Communications in Heat and Mass Transfer, 122: 105148. https://doi.org/10.1016/j.icheatmasstransfer.2021.10514
- [38] Promvonge, P. (2008). Thermal augmentation in circular tube with twisted tape and wire coil turbulators. Energy Conversion and Management, 49: 2949-2955. https://doi.org/10.1016/j.enconman.2008.06.022
- [39] Feng, Z., Li, Z., Hu, Z., Lan, Y., Zheng, S., Zhang, Q., Zhouc, J., Zhang, J. (2023). Combined influence of rectangular wire coil and twisted tape on flow and heat transfer characteristics in square mini-channels. International Journal of Heat and Mass Transfer, 205: 123866. https://doi.org/10.1016/j.iiheatmasstransfer.2023.12386
 - https://doi.org/10.1016/j.ijheatmasstransfer.2023.12386
- [40] Abbaspour, M., Mousavi Ajarostaghi, S.S., Hejazi Rad, S.A.H., Nimafar, M. (2021). Heat transfer improvement in a tube by inserting perforated conical ring and wire coil as turbulators. Heat Transfer, 50(6): 6164-6188. https://doi.org/10.1002/htj.22167
- [41] ASME. (1984). Standard Measurement of Fluid Flow in Pipes Using Orifice, Nozzle and Venturi. ASME, New York.
- [42] Kline, S.J., McClintock, F.A. (1953) Describing uncertainties in single-sample experiments. Mechanical Engineering, 75(1): 3-8.
- [43] Nanan, K., Thianpong, C., Pimsarn, M., Chuwattanakul, V., Eiamsa-ard, S. (2017). Flow and thermal mechanisms in a heat exchanger tube inserted with twisted crossbaffle turbulators. Applied Thermal Engineering, 114: 130-147.

- https://doi.org/10.1016/j.applthermaleng.2016.11.153
- [44] Syam Sundar, L., Singh, M.K., Punnaiah, V., Sousa, A.C.M. (2018). Experimental investigation of Al₂O₃/water nanofluids on the effectiveness of solar flat-plate collectors with and without twisted tape inserts. Renewable Energy, 119: 820-833. https://doi.org/10.1016/j.renene.2017.10.056
- [45] Chingtuaythong, W., Promvonge, P., Thianpong, C., Pimsarn, M. (2017). Heat transfer characterization in a tubular heat exchanger with V-shaped rings. Applied Thermal Engineering, 110: 1164-1171. https://doi.org/10.1016/j.applthermaleng.2016.09.020
- [46] Keklikcioglu, O., Ozceyhan, V. (2016). Experimental investigation on heat transfer enhancement of a tube with coiled—wire inserts installed with a separation from the tube wall. International Communications in Heat and Mass Transfer, 78: 88-94. https://doi.org/10.1016/j.icheatmasstransfer.2016.08.02
- [47] Eiamsa-ard, S., Nivesrangsan, P., Chokphoemphun, S., Promvonge, P. (2010). Influence of combined nonuniform wire coil and twisted tape inserts on thermal performance characteristics. International Communications in Heat and Mass Transfer, 37(7): 850-856. https://doi.org/10.1016/j.icheatmasstransfer.2010.05.01
- [48] Hong, Y., Du, J., Wang, S., Huang, S.M., Ye, W.B. (2018). Heat transfer and fluid flow behaviors in a tube with modified wire coils. International Journal of Heat Mass Transfer, 124: 1347-1360. https://doi.org/10.1016/j.ijheatmasstransfer.2018.04.017
- [49] Kola, P.V.K.V., Pisipaty, S.K., Mendu, S.S., Ghosh, R. (2021). Optimization of performance parameters of a double pipe heat exchanger with cut twisted tapes using CFD and RSM. Chemical Engineering & Processing: Process Intensification, 163: 108362. https://doi.org/10.1016/j.cep.2021.108362
- [50] Veza, I., Spraggon, M., Fattah, I.M.R., Idris, M. (2023). Response surface methodology (RSM) for optimizing engine performance and emissions fueled with biofuel: Review of RSM for sustainability energy transition. Results in Engineering, 18: 101213. https://doi.org/10.1016/j.rineng.2023.101213
- [51] Li, S., Qian, Z., Wang, Q. (2023). Optimization of thermohydraulic performance of tube heat exchanger with L twisted tape. International Communications in Heat and Mass Transfer, 145: 106842. https://doi.org/10.1016/j.icheatmasstransfer.2023.10684
- [52] Arjmandi, H., Amiri, P., Saffari Pour, M. (2020). Geometric optimization of a double pipe heat exchanger with combined vortex generator and twisted tape: A CFD and response surface methodology (RSM) study. Thermal Science and Engineering Progress, 18: 100514. https://doi.org/10.1016/j.tsep.2020.100514
- [53] Al-Obaidi, A.R. (2024). Investigation of the hydraulic performance heat improvement in 3D pipe by variable of novel twisted tape configurations based on CFD and DoE analysis methods. International Journal of Heat and Fluid Flow, 110: 109581. https://doi.org/10.1016/j.ijheatfluidflow.2024.109581
- [54] Yadav, M., Sawant, S. (2019). Effect of oxy-hydrogen blending with gasoline on vehicle performance

- parameters and optimization using response surface methodology. Journal of the Chinese Institute of Engineers, 42(7): 553-564. https://doi.org/10.1080/02533839.2019.1638305
- [55] Kumar, S., Dinesha, P. (2018). Optimization of thermal parameters in a double pipe heat exchanger with a twisted tape using response surface methodology. Soft Computing, 22: 6261-6270. https://doi.org/10.1007/s00500-018-3374-8
- [56] Kutner, M.H., Nachtsheim, C.J., Neter, J., Li, W. (2005). Applied Linear Statistical Models, Fifth Edition. London: McGraw-Hill Publication.
- [57] Kaood, A., Fadodun, O.G. (2022). Numerical investigation of turbulent entropy production rate in conical tubes fitted with a twisted-tape insert. International Communications in Heat and Mass Transfer, 139: 106520. https://doi.org/10.1016/j.icheatmasstransfer.2022.10652
- [58] Al Qudah, S., Radwan, A., El-Sharkawy, I.I. (2025). Experimental analysis of heat transfer in a circular tube fitted with new twisted tape insert with rings using response surface methodology. International Journal of Heat and Fluid Flow, 112: 109713. https://doi.org/10.1016/j.ijheatfluidflow.2024.109713
- [59] Anderson, M.J., Whitcomb, P.J. (2017). RSM Simplified
 Optimizing Processes Using Response Methods for Design of Experiment, Second Edition. New York: CRC Press, Taylor and Francis.

NOMENCLATURE

A_s	Surface area of the tube, m ²
CCD	Central composite design
CLR	Conical length ratio
CorTotal	Corrected total sum of squares
C_p	Specific heat of water at constant pressure,
•	$J.Kg^{-1}.K^{-1}$
d	Diameter of the tube, m
df	Degrees of freedom
DR	Diameter ratio
f	Friction factor
h	Heat transfer coefficient, W.m ⁻² .K ⁻¹)
1	Length of the tube, m
m	Mass flow rate of water, Kg.sec ⁻¹
Model SS	Model sum of squares
Nu	Nusselt number
PR	Predicted response
Pr	Prandtl number
\mathbb{R}^2	Coefficient of determination
Re	Reynolds number
T_b	Mean bulk temperature, K
T_{in}	Temperature of water at inlet, K
T_{out}	Temperature of water at outlet, K
T_s	Mean surface temperature, K
v	Velocity of water, m.sec ⁻¹
Δp	Pressure drop in the test section, N.m ⁻²

Greek symbols

ρ Density of water, Kg.m⁻³

Subscripts

b Bulk s Surface

Superscripts

INV Inverse T Transpose

APPENDIX

Appendix-I

Calculations involved in ANOVA and RSM

To model the experimental results, three matrices are used: the matrix of model terms [A], the matrix containing the regression coefficients [B] and the response matrix [C]. These three matrices are related by Eq. (26).

$$[A] \times [B] = [C] \tag{26}$$

To simplify the regression analysis and interpretation, the model terms were converted into coded form, assigning +1 to the highest level and -1 to the lowest level. Intermediate levels are coded using equal intervals within the specified range. In order to obtain model term coefficients, the matrix operations given by Eq. (27) are performed [56].

$$[B] = [A^T A]^{INV} \times [A^T C] \tag{27}$$

where, superscripts *INV* and *T* denote inverse and transpose operations of a matrix, respectively.

The corrected total sum of squares (*CorTotal*) in the *ANOVA* is obtained by using Eq. (28).

$$CorTotal = \sum_{i=1}^{n} y_i^2 - Z^2/N$$
 (28)

where, y_i is the actual response (AR). The variable Z denotes the addition of all measured values of the response variable. and N is the value of the total count of experiments. Using model Eqs. (17)-(22), predicted responses (PR) are obtained. Then the residual is obtained by using Eq. (29).

$$Residual = \sum_{i=1}^{N} (AR_i^2 - PR_i^2)^2$$
 (29)

The model sum of squares (*Model SS*) is calculated by deducting the residual from the corrected total sum of squares (*CorTotal*). It is given by Eq. (30).

$$Model SS = CoTotal - Residual$$
 (30)

The factor sum of squares is obtained by excluding each model term individually from the model term matrix [A]. Accordingly, the coefficient matrix [B] is adjusted. New model term coefficients and model equations are obtained by repeating all matrix operations described in Eq. (27). For each model term, a new residual sum of squares is computed by excluding the term from the model. The difference between this and the residual from the complete model represents the sum of squares for the removed term. This procedure is repeated for each remaining model term to compute its respective SS values.

Total degrees of freedom (df) in the ANOVA table is calculated by subtracting one from the total number of experiments. Each model term is allocated one degree of freedom. As there is a total of nine terms, the value of df for the model is nine. The residual df is calculated by subtracting the total model df from the total df. Mean square (MS) is obtained by dividing SS by the respective df. The F-value is computed by taking the ratio of the mean square associated with the independent variable to the mean square of the residual error. The confidence level (CL) and p-value for the model are derived from the F-distribution, utilizing the model's F-statistic along with its associated degrees of freedom for both the model and the residuals.